STATISTICAL CHARACTERIZATION OF ATMOSPHERIC PRESSURE DIELECTRIC BARRIER DISCHARGE

R.A. SILIPRANDI, H.E. ROMAN, R. BARNI AND C. RICCARDI

Dipartimento di Fisica "G. Occhialini", Università degli Studi di Milano-Bicocca, Piazza della Scienza 3, 20126 Milano, Italy

We investigate the statistical properties of a typical dielectric barrier discharge in a streamer regime. To this end, we develop and calibrate a wide bandwidth Rogowski coil probe able to resolve nanosecond current pulses. We study global quantities such as the transferred total charge in a discharge process and the associated current response. We find two distinct discharge regimes as a function of the applied external voltage, which are identified by the behavior of the first moments of the discharge current. The corresponding probability distribution functions are obtained.

Key words: atmospheric pressure plasma, dielectric barrier discharge (DBD), streamers, statistical analysis.

1 Introduction

Dielectric barrier discharges (DBDs) at atmospheric pressure are a well known type of gas discharge. They have been widely used in industrial applications like ozone generators, plasma display panels, excimer lamps and surface modifications [1-4]. Usually, in a streamer regime, individual microdischarges compete for the available surface area of the dielectric to deposit their charge patterns and, under specific conditions, their strong interaction can lead to the formation of coherent spatial configurations that have been widely observed in different types of experimental setups [4-6]. Yet, in most applications of DBDs operating in a streamer regime the microdischarges seem to randomly occur in the discharge gap.

In this work, we investigate the temporal behavior of current pulses for a streamer regime of a DBD in atmospheric air. To our knowledge the statistical properties of such discharges have not been discussed with sufficient insight in literature so far, even if some efforts in this direction have been made to explain some features of partial discharges [7]. In particular, using a statistical analysis, we find two different behaviors of the discharge depending on the external applied voltage. The separation between these two regimes can be identified by looking at several statistical properties of the current signal.

2 Experimental Setup

Figure 1 shows a schematic diagram of the experimental setup. Both the current and the voltage are acquired in a Nicolet Multipro oscilloscope, respectively, with specific designed Rogowski coils [8,9] and a high voltage probe (Tektronix P6015A). Using a calibration system [9] we determine the amplitude response, the phase shift and the sensitiveness of the Rogowski coils.

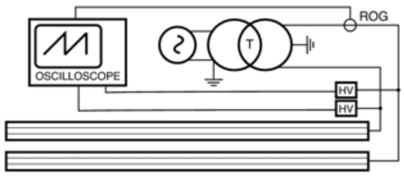

Fig. 1: DBD device : two rod electrodes 290 mm long and 15 mm square section ceramic dielectric. Distance between electrodes is 4 mm. An amplified signal generator, (31÷36) kHz, and a current transformer (T) provide the high voltage to the electrodes.

The amplitude-frequency and phase-shift-frequency response determined with a calibration system [9] of the present Rogowski coils are plotted in Fig. 2. The responses of the two types of coils to the shortest current pulses in the device were found to be almost undistinguishable to each other. Therefore, we choose to use the lower bandwidth coil because it has a lower amplitude loss in the range of the displacement current response of the system (see Fig. 2). The current signal is acquired with sampling time of 5 ns, yielding time series of $3 \cdot 10^5$ steps, for different applied peak-to-peak external voltages in the range (22÷26) kV.

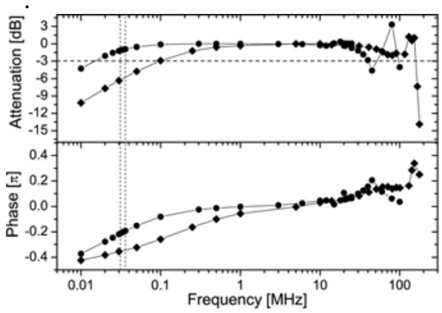

Fig. 2: Amplitude-frequency and phase-shift-frequency response of the Rogowski coils. (●) Represent a ferrite core coil with a 50 kHz-70 MHz bandwidth. (♦) NiZn core coil with a 400 kHz-120 MHz bandwidth. Vertical dotted lines represent the frequency range of the displacement current.

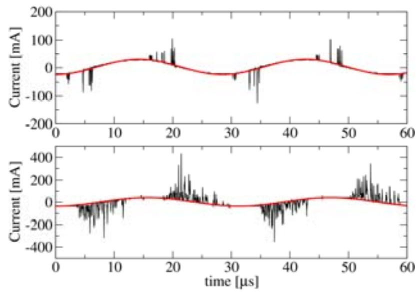

Fig. 3: Typical current signal of a DBD device. The upper and lower figure refer to a low voltage and high voltage current signal, respectively, typical of the two behaviors of the discharge observed in the device. The sinusoidal continuous line is the fitted displacement current of the system.

3 Results and discussion

The total current can be decomposed into a sinusoidal displacement current, which does not depend on the presence of plasma in the gap, plus the current response due to the discharge process [10], which we denote as I(t). An example of the signal and the fitting sinusoidal function are shown in Fig. 3. We have verified that both positive and negative discharge currents essentially obey the same statistics, i.e. their probability distribution functions are almost indistinguishable from each other. In order to improve the statistics, we change the sign of the negative half-period currents and consider them together with the positive half-period ones. Here we use a cutoff $I_{cut} \cong 10$ mA below which I(t) is taken as zero. In our analysis, we consider values of I(t) only within an effective time interval $t_{min}<t<t_{max}$, for a fixed applied voltage V_{pp}. For each bump the current is indicated as $I_B(t)$ and t_{min} (t_{max}) is defined as the lowest (highest) time within a half-cycle at which I(t)>0. The total number of bumps, N_B, is typically $N_B \cong 100$, while Δt=tmax-tmin varies in the range 6 μs <Δt<11 μs, depending on V_{pp}. The mean response function, $\langle I_B \rangle$, is obtained by averaging I_B over the hundred periods registered in the time series.

In the lower panel of Fig. 4 a typical discharge current signal $I_B(t)$ is represented within a half cycle, which we denote as a discharge bump or simply bump. It can be noted that a bump is composed of several well separated discharge bunches, which we call bursts. The bursts are made of a series of consecutive and overlaping streamers which get clustered together. In the upper-left panel of Fig. 4 the probability density function (PDF) of $I_B(t)$ is plotted. It shows that during most of the time the discharge process is inactive while the activity can be approximated by an exponential PDF which is typical of non correlated avalanche processes. In the upper-right panel of Fig. 4 it is represented the variation of the decay parameter λ as a function of V_{pp}. If we consider that the charge transported by a single streamer is not affected by the applied voltage [4], a high current signal indicates that a high number of microdischarges are initiated almost simultaneously. In the low voltage regime not all the available space on the dielectric is filled with streamers. By increasing the applied voltage, additional microdischarges can be generated giving rise to a rapid growth of λ. As long as the maximum number of simultaneous streamers is reached, the second, high voltage regime starts and λ remains almost constant. In this case only the number of bursts, i.e. the percentage of activity of the discharge duration, increases.

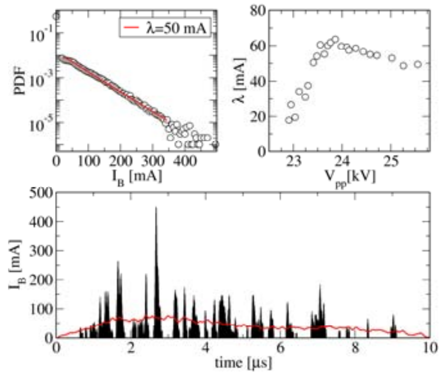

Fig. 4: Lower panel: discharge current signal $I_B(t)$ of a high voltage (V_{pp}=25.3 kV) discharge plotted within t_{min} and t_{min} The continuous line is the mean response $<I_B(t)>$. Upper left panel: PDF of $I_B(t)$, the continuous line represents: $P(I_B)\propto\exp(-I_B/\lambda)$. Upper right panel: parameter λ as a function of V_{pp}.

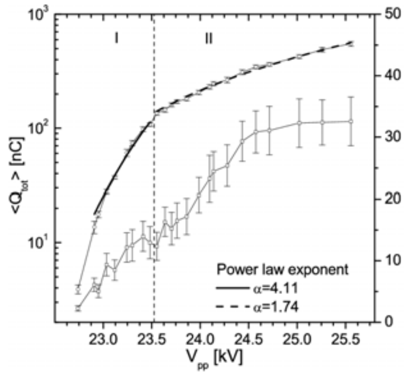

Fig. 5: Upper curve: $<Q_{tot}>$ as a function of V_{pp}. Continuous and dotted lines are power laws plotted as guidelines : $<Q_{tot}>\propto(V_{pp})^{\alpha}$. Lower curve: mean value of the number of current bursts $<N_b>$. Here, $Q_{tot}=\int_{t_{\min}}^{t_{\max}} I_B(t)dt$.

An important quantity related to the efficiency of the discharge device is the total charge transferred each half period by the system (see Fig. 5), also revealing again two distinct behaviors. Below $V^c_{pp}\cong$23.5 kV the increase of $<Q_{tot}>$ (mean over bumps) is faster probably because the streamers can develop without strongly interfering neither in space nor in time. For voltages larger than V^c_{pp}, the rate at which charge increases becomes slower and higher powers are needed to rise $<Q_{tot}>$ further. From $I_B(t)$ we can also calculate the number of current bursts generated during the single discharge process (Fig. 5). We can see that the mean number of bursts $<N_b>$ (mean over bumps) is slightly more noisy than the total charge $<Q_{tot}>$, displaying an initial linear behavior as a function of voltage followed by a much slowly dependence at higher values of V_{pp}, probably because bursts tend to overlap and their number gets underestimated.

The two discharge regimes can also be observed in two additional quantities: burst length τ_δ and the quiet (or waiting) time τ_w. The former is defined as the duration of the activity of the system (i.e. the time length of a single current burst), the latter is defined as the inactivity interval between the bursts. Both quantities are considered only inside bumps. The PDF and their moments for these quantities can be calculated for each value of V_{pp}. The first two moments of burst lengths (Fig. 6) increase rapidly to a limiting value when they reach V^c_{pp}. This could be explained by the limited number of simultaneous streamers the system can generate because of their competing interaction [4]. Their further increase at higher values of V_{pp} can be explained as an effect of overlap between bursts already observed in the behavior of N_b (Fig. 5). The higher moments (third and fourth ones) can tell us about the shape of the PDF and in Fig. 6 they are compared with those from an exponential PDF. Clearly, the exponential behavior is not enough to explain the observed PDFs completely. In Fig. 7 the first four moments of the quiet time intervals τ_w are plotted. The mean value $<\tau_w>$ and standard deviation σ_w rapidly decrease with increasing voltage, reaching a minimum value around V^c_{pp} after which they decrease more slowly.

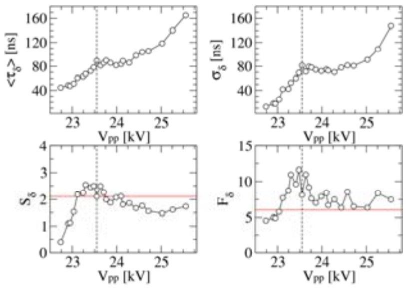

Fig. 6: First moments of the burst lengths τ_δ versus applied voltage V_{pp} [kV]. Shown are: the mean value $<\tau_\delta>$, standard deviation σ_δ, skewness S_δ and flatness F_δ. The horizontal line represents the values of S and F for an exponential PDF. Vertical dashed line is the separatrix value $V^c_{pp} \cong 23.5$ kV.

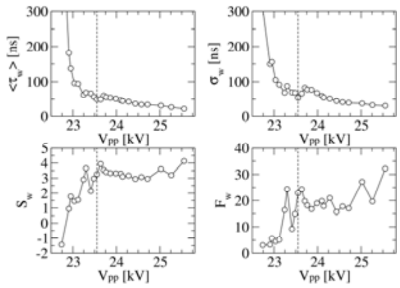

Fig. 7: First moments of the quiet times τ_w versus applied voltage V_{pp} [kV]. Shown are: the mean value $<\tau_w>$, standard deviation σ_w, skewness S_w and flatness F_w. The vertical dashed line indicates the separatrix value $V^c_{pp} \cong 23.5$ kV.

The quantity τ_w represents the time needed by the system to recreate the discharge condition. As long as the streamers can occur without strong interaction (as in the low voltage regime) τ_w can vary rapidly with the power furnished to the system. When the interaction between simultaneous streamers starts to limit their number, and all the dielectric is filled with microdischarges, the recreation of discharge conditions can be obtained by rising the external voltage. This fact is stressed by the behavior of $<\tau_w>$ and σ_w. Their slow decrease at higher voltages is probably related to the increase of dV_{pp}/dt. The higher moments of the distribution show unconventional behavior with respect to Gaussian or exponential distributions.

4 Conclusions

We have presented preliminar results concerning the characterization of dielectric barrier discharges at atmospheric pressure. Using statistical tools we have analyzed a DBD discharge in air as a function of the applied voltage. In particular we have found two different discharge regimes and we have characterized them by analyzing several quantities related to the discharge current. Both regimes are distinguished by the different dependences on applied voltage of the quantities studied, the latter varying much stronger in the low-voltage regime. Also the bursts dynamics and shape are different, in the low-voltage regime bursts are of short duration and made of few streamers, while in the high-voltage one bursts get longer in time and have higher intensity. In the latter, bursts reach a typical shape and discharge current can further increase only by increasing the number of bursts.

References

[1] K. Becker, U. Kogelschatz, K. Schoenbach, and R. Barker, Non-Equilibrium Air Plasmas at Atmospheric Pressure (Institute of Physics Publishing, 2004).
[2] U. Kogelschatz, Plasma Chemistry and Plasma Processing 23, 1 (2003).
[3] B. Eliasson and U. Kogelschatz, Plasma Science, IEEE Transactions on 19, 309 (1991).
[4] U. Kogelschatz, Plasma Science, IEEE Transactions on 30, 1400 (2002).
[5] L. Stollenwerk, S. Amiranashvili, J.-P. Boeuf, and H.-G. Purwins, Phys. Rev. Lett. 96, 255001 (2006).
[6] J. Guikema, N. Miller, J. Niehof, M. Klein, and M. Walhout, Phys. Rev. Lett. 85, 3817 (2000).
[7] R. J. Van Brunt, P. von Glahn, and T. Las, Journal of Applied Physics 81, 840 (1997).
[8] M. Argueso, G. Robles, and J. Sanz, Review of Scientific Instruments 76, 065107 (pages 7) (2005).
[9] Q. Zhang, J. Zhu, J. Jia, F. Tao, and L. Yang, Measurement Science and Technology 17, 895 (2006).
[10] F. Massines et al,, Plasma Physics and Controlled Fusion 47, B577 (2005).
[11] Y. P. Raizer, Gas discharge physics (Springer, 1997).